Scientific Research and Essays Vol. 7(43), pp. 3682-3689, 5 November, 2012
Available online at http://www.academicjournals.org/SRE
DOI: 10.5897/SRE11.1489
ISSN 1992-2248 ©2012 Academic Journals

Full Length Research Paper

Study on ringing effect in ultrasonic transducer

M. S. Salim[1]*, M. F. Abd Malek[2], Naseer Sabri[3] and K. M. Juni[4]

[1]School of Mechatronics Engineering, University Malaysia Perlis, Kangar, 01000, Malaysia.
[2]School of Electrical System Engineering, University Malaysia Perlis, Kangar, 01000, Malaysia.
[3]School of Computer and Communication Engineering, University Malaysia Perlis, Kangar, 01000, Malaysia.
[4]Electrical Engineering Department, Politeknik Tuanku Syed Sirajudain, Malaysia.

Accepted 7 June, 2012

This paper presents theoretical experimental and evidence of the effect of internal resonance at silicon substrate in micro fabrication ultrasonic transducer. This ringing is clearly observed in immersion transducers with 4.2 MHz and harmonics. A mathematical analytical model of the attenuation yield by ringing effective and simulation is introduced. Experimental results are further compared to simulations carried out in time-domain and qualitative agreement is provided. This paper summarizes the theoretical measured, performance backing layer. Experiment and simulation proved that it is possible to design a custom backing material with acoustic impedance that decreases the ringing mode.

Key words: Capacitive micro-machined ultrasonic transducers (CMUT), ultrasound sensor, backing layer, attenuation.

INTRODUCTION

Miniaturization capability of the silicon micromachining process made the fabrication of devices working at ultrasonic frequencies possible. These devices are called capacitive micro-machined ultrasonic transducers CMUTs. CMUTs are made of small and thin membranes that are suspended over a conductive silicon substrate by insulating posts. CMUTs are usually operated under a direct current (DC) bias, where the DC electrostatic forces attract the membrane toward the substrate to a point where the total electrostatic force is balanced by the stiffness of the membrane. The diameter of the membrane ranges from 10 mm to hundreds of micrometers. The gap between the membrane and the substrate is vacuum sealed or left unsealed at will and it can be as small as 500 Å. The membranes are either conductive or coated with a conductive electrode and essentially create small capacitors together with the substrate. This structure results in very efficient transducers that can compete with their piezoelectric counterparts in terms of efficiency and bandwidth. The CMUT can be used both for emitting and receiving ultrasound. This is done by either driving the membrane vibration by an AC signal for emission, or receiving by measuring the variation in deflection when pressure variations is induced on the membrane by the medium. Common for both modes is that it needs to have a bias voltage in order to work properly. Due to the unipolar nature of electrostatic attraction, a qualitatively assessment would suggest that unless the CMUT is biased, the membrane would vibrate at double frequency compared to the driving signal. This is also shown through equations (1) and (2) by looking at the CMUT as a parallel plate capacitor where the suspended electrode can move without being deformed. Another assumption that will be made for these equations is that electric fringe fields can be ignored. From Liu (2006) we can derive the unipolar electrostatic force between the plates in the capacitor as equal to the absolute gradient of the stored energy (U) with respect to the variable distance (d). Equation (1) shows that the force is to be proportional to E^2, and by taking

$$F_{electric} = \frac{|\partial U|}{|\partial d|} = \frac{1}{2}\frac{|\partial C|}{|\partial d|}V^2 \quad (1)$$

into account that the electric field has two contributors, E_{DC} and E_{AC} , an expression for E can be written:

*Corresponding author. E-mail: muhsabri1967@yahoo.com.

$$E^2 = E_{DC}^2 + 2E_{DC}E_{sig}COS(wt) + E_{sig}^2 COS(wt)^2 \quad (2)$$

Where V is the potential over the plates, Ɛ is the permittivity of the media and A is the area of the plate. Setting the DC component in (2) to zero results in a vibration frequency which twice as high as the driving signal. Biasing is therefore needed, and it also shows that E_{DC} needs to be larger than E_{sig} for the device to operate in a linear regime where it can be analyzed without having a complete under-standing of its behavior (Ladabaum et al., 1998). When the CMUT is used for receiving acoustic waves, the vibrations in the membrane are detected by measuring the variation in capacitance. A constant bias voltage is needed so that this variation in capacitance induces a current that the receiving circuitry can read. This paper illustrates the measurements and analysis of the performance of the added backing layer. All of the data presented in this paper is programmed in MATLAB (Delund, 2010), and laboratory experiment.

Attenuation in fluid

For an ultrasonic wave traveling through a material, the energy of the wave will bleed off as the wave propagates. This mean its amplitude will decrease. The main reasons for this are absorption and scattering (Martini et al., 2005), which adds up over the distance traveled. Other transmission losses like reflection and refraction of the wave (Kocis, 1996) also occur. Absorption in fluids occurs as a result of the viscosity of the fluid, which is a measure of the fluids resistance to shear and tensile stresses. This resistance causes a conversion of ultrasonic energy into other forms, and will eventually dissipate it as heat (Raichel, 2006; Martini et al., 2005). The attenuation coefficient (α) for fluid can be expressed as Kocis (1996).

$$\alpha = \frac{8\pi^2 \eta F^2}{3\rho c^3} = \alpha_o f^2 \quad (3)$$

In expression (3), η denotes dynamic viscosity, is the density, and c is the speed of sound in the fluid. This expression only considers dynamic/shear viscosity. This has however been shown to give considerably smaller values compared to attenuation measurements. The main points to note about these expressions are:

1. The relation $\alpha \infty f^2$, which means that attenuation, increases quadratically for increasing frequencies;
2. Temperature dependencies;
3. The volume viscosity is related to a lag in flow of the fluid when experiencing acoustic pressure. This lag causes attenuation because the fluid cannot keep up with the compression/expansion rate demanded at higher frequencies; and
4. Scattering also contributes to the attenuation, especially in heterogeneous media where there are many particles that can interact with the wave. The size and concentration of these particles will affect the degree of attenuation contributed by scattering (Kocis, 1996).

In addition to attenuation, transmission losses due to reflection/transmission and refraction can also add to the total loss of energy for a received wave. When a wave encounters a boundary between two media, a part of it will be reflected and the rest is transmitted into the second medium depending on the acoustic impedances of the media. If the wave transmitted into the second medium is not reflected back later, the energy transmitted can be considered lost. Refraction of the wave also contributes to higher losses in certain cases because the propagation direction changes. This is the case when a receiver picks up only a part of the wave or nothing at all, due to this change (Delund, 2010).

Silicon substrate ringing effect

During generation of ultrasound, waves will be emitted into the measuring medium, but also internally in the CMUT substrate. This internal resonance will add a ringing effect to the emitted pulse and increase the duration of the emitted pulse. This leads to a decrease in resolution and also sensitivity since ringing reduces the instantaneous intensity of the emitted pulse (Hedrick, 2004). With less instantaneous intensity reflections from poorly reflecting surfaces will not be detectable. It is therefore desirable to add a backing material to absorb the energy in the substrate, and by this reduce ringing, that is, the number of cycles in the emitted pulse. Therefore the performance of the transducer for diagnostic imaging will be improved.

For maximum transfer of energy to occur, the acoustic impedance of the backing should be identical to that of the transducer, which can be seen from the relations of reflection and transmission (Delund, 2010), where a transmission coefficient at unity would be ideal. The backing material is usually made of an epoxy resin/composite mixed with tungsten powder (Hedrick, 2004). This compound's main absorption mechanism is conversion to heat by scattering of the ultrasonic waves by the tungsten particles. Due to the equal impedances of the transducer and backing material, transmission back into the transducer can occur if the absorption is not great enough. This can be avoided by having a slanted rear side of the backing, which will refract the ultrasonic waves away from the transducer (Kocis, 1996; Hedrick, 2004).

METHODS

When performing characterization measurements, whether it is pulse-echo, transmission measurements or pitch-catch method, the initial results one will obtain is characteristic for the system as a whole, and not for the tested device itself. In order to get a better

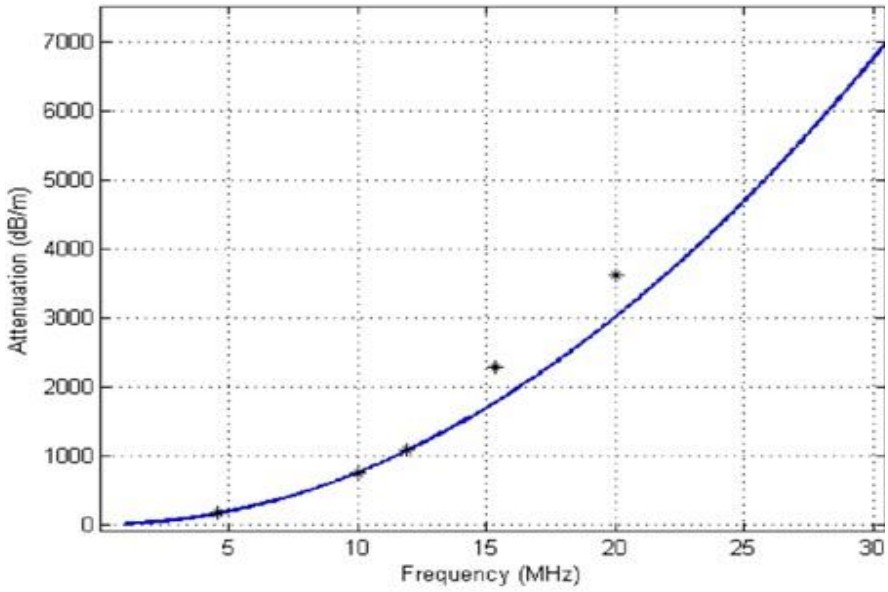

Figure 1. Theoretical attenuation versus frequency (Delund, 2010).

impression of the performance of the tested device, variables in the system will have to be accounted and compensated for.

Attenuation in the measuring medium is one of the main variables that affect the initial result, especially since it varies as a function of frequency (Delund, 2010). Finding the attenuation of the medium that the measurements are performed in, in this case, rapeseed oil is therefore needed to produce a normalized response curve for the CMUT. In the data on the rapeseed oil, a value for the volume viscosity is not stated. Therefore, this equation is suspected to give smaller values than the actual ones. A measurement of the attenuation is therefore needed to produce a correction curve, and not only validating and adjusting of theoretical one.

Theoretical and experimental measured rapeseed attenuation

Figure 1 illustrates the theoretical relation between the attenuation and frequency, which is calculated using (3), with dynamic viscosity = 72.1 mPa.s, density = 910 kg/m^3, propagation velocity, c = 1460 m/s. The measurement of rapeseed attenuation can be done using network analyzer method or by Olympus pan metrics method, but each of the methods has their weaknesses that can be a source of uncertainty in the measurements.

Network analyzer method: Skewed alignment of the transducer, this yield greatest uncertainty source. The measurement of the two positions is also subject to some uncertainty.

Olympus method: The propagation speed c is the source of greatest uncertainty It was found by measuring the placement of the first echo in time at two different positions.

The measurement series were performed six times for each method to have a set of values to average over. This was done to even out the uncertain-ties of the measurements. The averaging was also weighted, meaning that the largest deviations were essentially excluded. The system is inherently loss, and the measurements with the lowest losses can therefore be considered to be closer to the real value than those with higher values. This does not mean that picking out the lowest value for each frequency will be acceptable, since for example a value for c that is too high gives attenuation values that are too low. Both methods gave values in the same range of attenuation values for each frequency, and they were therefore processed together in the calculation of data points. Figure 2 shows the plotted data points representing the averaged values for specific frequencies, and the adapted curve for the attenuation as a function of frequency. More weight have also been put to the lower frequencies since the attenuation is lower here, and measuring errors will have less effect compared to the higher frequencies. The significance of this can be seen in Figure 2 where the curve follows the lower frequency values closer compared to the values at higher frequencies. This corresponds to with

$$\alpha = 7.5\times10^{-12}\,\frac{dB}{m}S^2 \qquad (4)$$

this is about 1.3 times greater than the theoretical value. The experiment was repeated 5 times to be used as the extra data point seen in Figure 2. The actual attenuation turned out to be higher than the theoretical value, as expected from the theory. The result is also a comparable value with the results presented in Delund (2010), and Coupland and Mcclements (1997), on similar vegetable oils. The main source of the increased attenuation, compared to the theoretical one, is probably the effects added by the volume viscosity, assuming the oil is homogeneous. It is however unlikely that the oil is completely free from some undissolved cells or other impurities, so scattering may be a contributor too.

Weidlinger finite element model

Foremost is the need for two distinct resolution scales, due to the thickness disparity between MUT structure (2 to 3 microns) and the silicon wafer (around 600 microns). Second is nonlinearity in both the electrical and mechanical fields. Weidlinger associates have developed a time domain finite element model that treats near-surface structure as a constrained boundary layer and includes all electromechanical coupling between individual membranes. It permits global 3D models, that is, “many” neighboring membranes

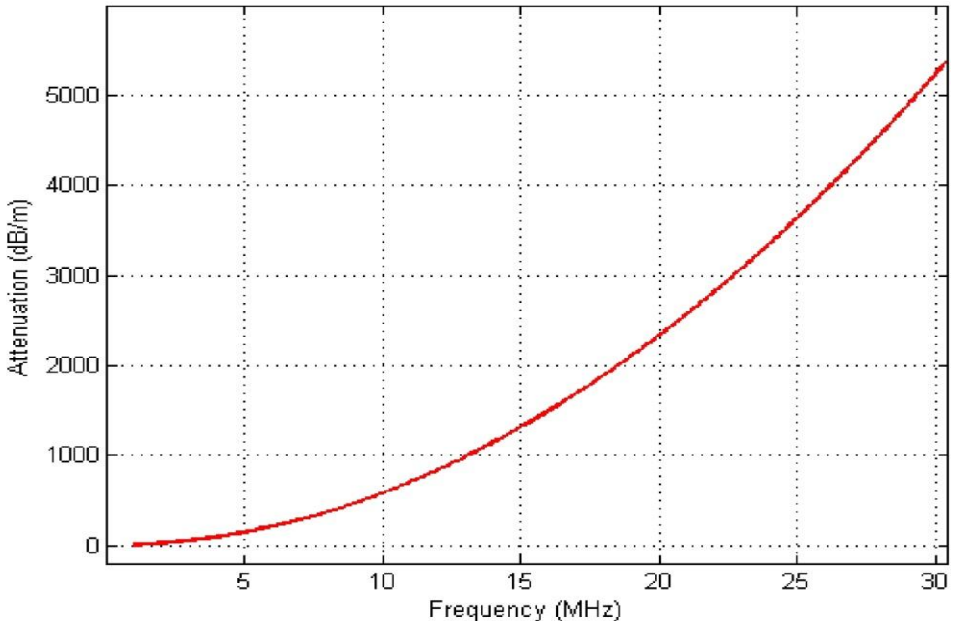

Figure 2. Averaged data points and adapted curve for the measured attenuation versus frequency (Delund, 2010).

over a significant piece of silicon real estate. This boundary layer model relies on a high-resolution, local model of MUT response for calibration of the membrane approximation (Wojcik et al., 2000).

RESULTS

In actual devices, the CMUT membrane is usually made of a dielectric material and the electrodes are formed by depositing a metal on top of the membrane. The effect of the membrane can be included by changing the gap height d_0 with the effective gap height d_{eff}, which is given by Ergun et al. (2003)

$$d_{eff} = \frac{d_m}{\varepsilon_r} + d_o \quad (5)$$

where d_m is membrane thickness and ε_r is relative dielectric constant of the membrane material.

In addition, the membrane capacitance is calculated using the following expression:

$$C(x) = \frac{A\varepsilon_o}{d_{eff} - x} \quad (6)$$

Equation (7) suggests a greater output for an increasing bias voltage, and it was found in Hansen et al. (2000), that the CMUT followed this pattern. As this was already established for the CMUT, the observation served to confirm that the CMUT functioned

$$k_T^2 = \frac{2x}{deff - x} \quad (7)$$

Properly, and still followed this pattern after the addition of the backing layer. The purpose of the backing layer is to reduce the ringing effect in the CMUT. This has been reported to be effective in Ladabaum (2000), and comparison with measurements from before the layer was added will show how it performs in this case. The initial frequency responses for the CMUT, without and with the backing layer added, are shown in Figures 3, 4, 5 and 6, respectively. The ripple in the response is expected in both cases, and corresponds to the distance from the reflector and the speed of sound in the rapeseed oil. The property of interest in these plots is able to design a custom backing material with an acoustic impedance that does indeed match that of silicon and loss which is sufficient to eliminate the ringing mode.

DISCUSSION

Pitch catch transmission method experiments was performed to first discover the ringing mode and then to prove that implementation of designed backing material exclude the ringing effect. FFT was used to get the frequency responses of the time-domain impulse response.

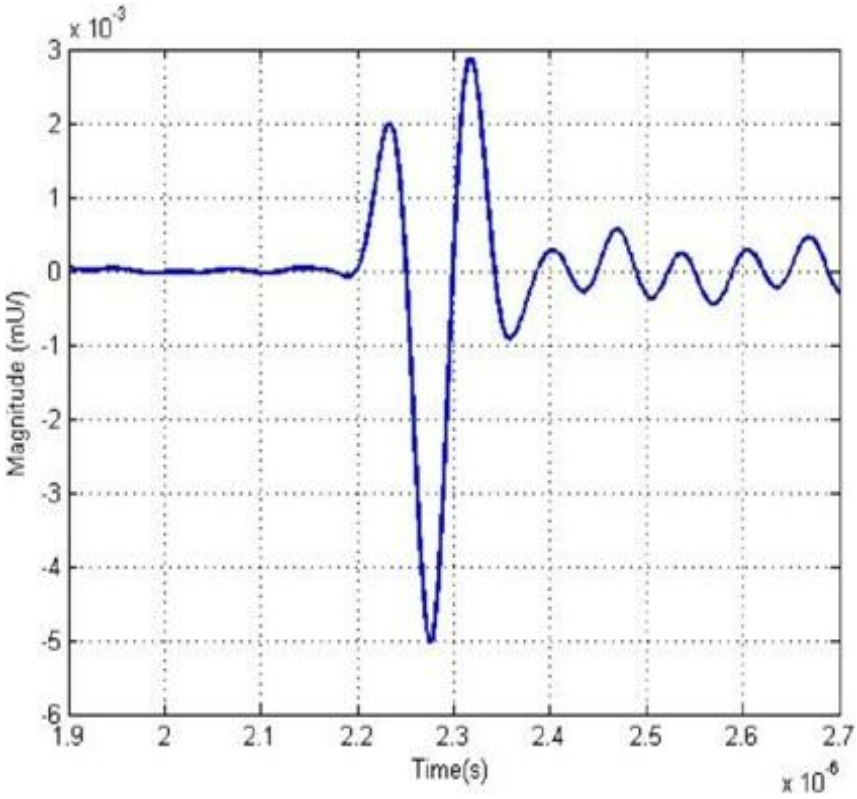

Figure 3. Simulated zoomed in impulse response of the first echo, without backing layer (Delund, 2010).

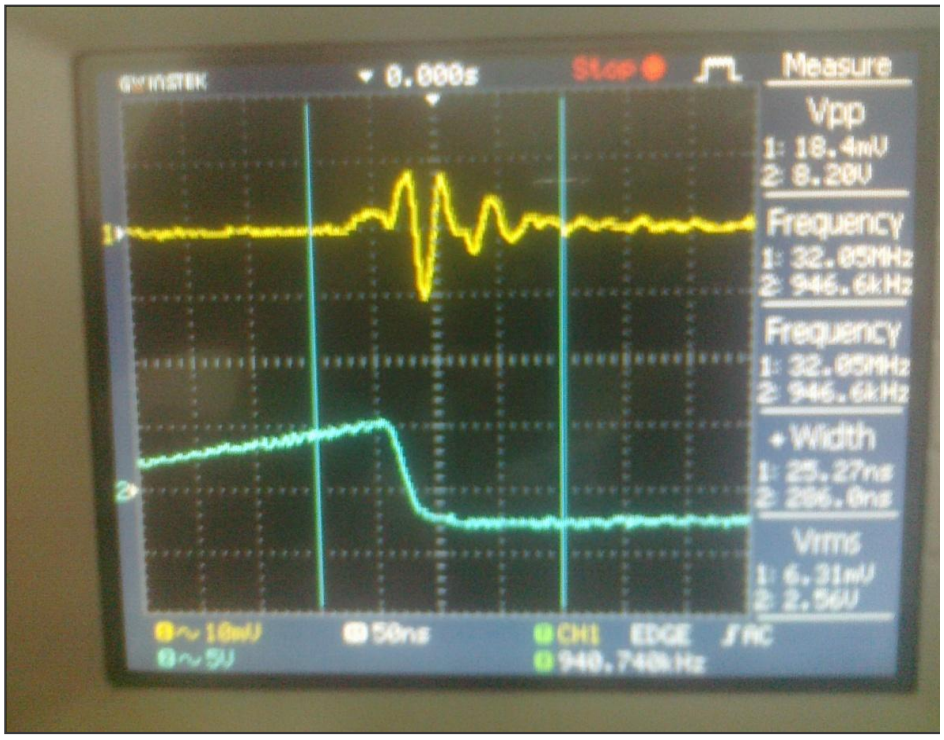

Figure 4. Experimental zoomed in impulse response of the first echo, without backing layer.

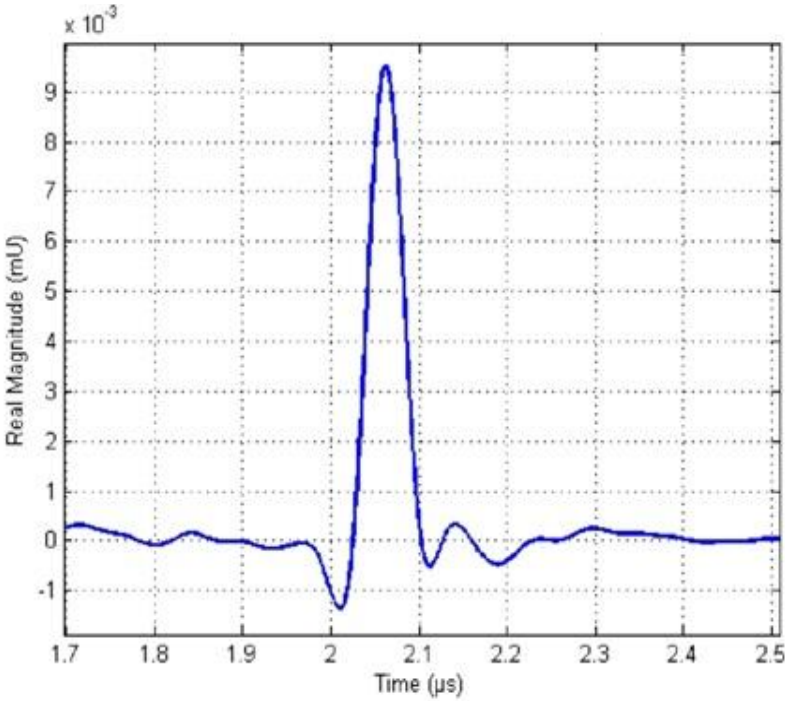

Figure 5. Simulated zoomed in impulse response of the first echo, with added backing layer (Delund, 2010).

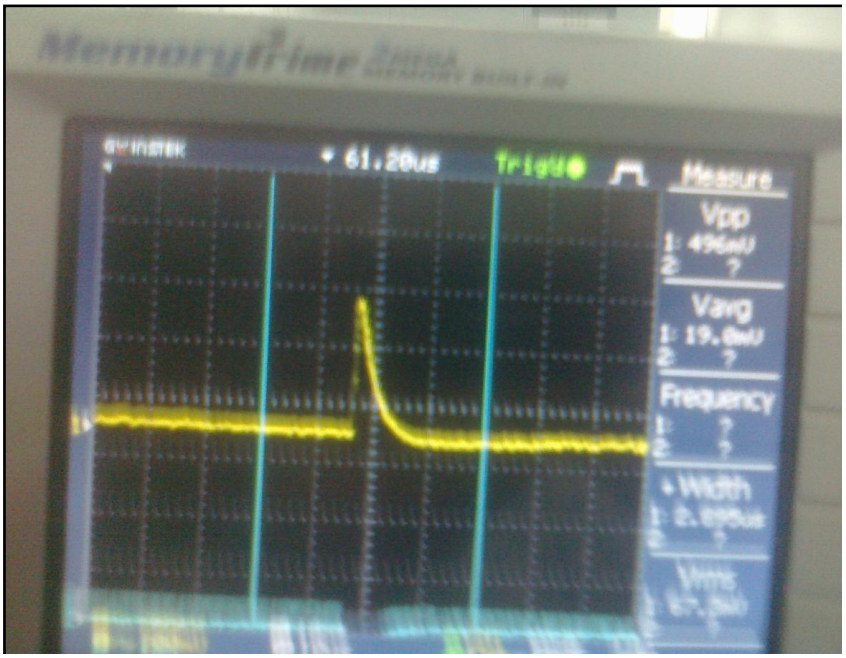

Figure 6. Experimental zoomed in impulse response of the first echo, with added backing layer.

A long ringing tail in the time domain was demonstrating the first transmission experiment. To develop the mechanical model, the observation of tail in the experiment must be provided. A zoomed section of the first echo for CMUT, with and without the backing layer, is shown in Figures 3, 4, 5 and 6, respectively. This

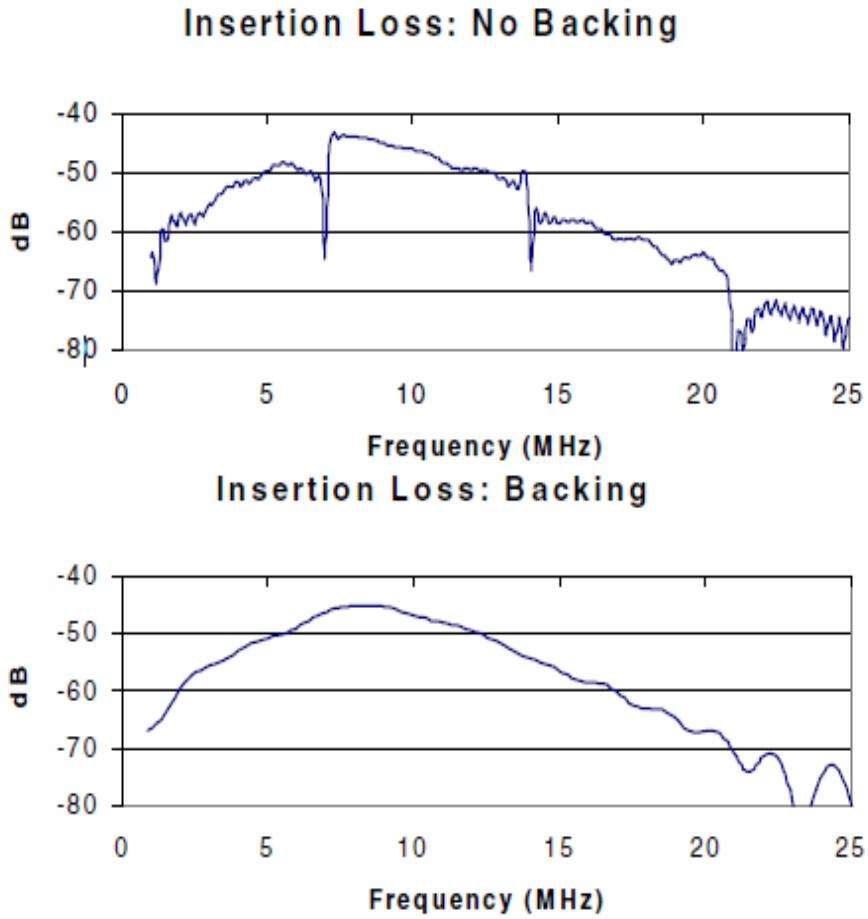

Figure 7. FEM simulation results (Wojcik et al., 2000).

confirms that the ringing is resonance internally in the CMUT chip as suspected in relation to Ladabaum et al. (2000), and Logan and Yeow (2009).

Figure 7 shows the results obtained from Weidlinger associates' time domain FEM (Wojcik et al., 2000), both with and without a backing material. The characteristic of backing material must have acoustic impedance matches that of silicon and that it must be very less. With these constraints, any acoustic amplitude reaching the back of the substrate would be dissipated, so ringing effect would be deleted. Greatly improved transducer performance with backing material is clearly shown in Figure 7.

Conclusion

The objective of this paper is to study the effect of attenuation generated by CMUT internally resonance and adding observe layer. Comparing the impulse responses with and without the backing layer, shows that the ringing is removed with adding backing layer. The dims that were present in the frequency response, has also been removed with the added backing. The attenuation is directly propositional to frequency square and the backing layer capture of CMUT depends on the absorption factor of the backing layer. FEM model for CMUT clearly describe the physics and can be used as estimation models. Finally, we have experimentally provided that the substrate ringing effect can be decreased by placing matched and attenuate backing material in contact with the silicon substrate. The advantages of this work are to modify the echoscope for high imaging resolution.

REFERENCES

Coupland JN, McClements DJ (1997). Physical properties of liquid edible oils. J. Am. Oil Chem. Soc. 74(12):1559–1564.

Delund P (2010). Evaluation of a Capacitive Micromachined Ultrasonic Transducer with backing layer. MSc. Thesis. Department of Electronics and Telecommunications, Norwegian University of Science and Technology.

Ergun AS, Yaralioglu GG, Khuri-Yakub BT (2003). Capacitive Micromachined Ultrasonic Transducers: Theory and Technology. J. Aerospace Eng. 16(2):76-84.

Hansen ST, Turo A, Degertekin FL, Khuri-Yakub BT (2000). Characterization of capacitive micromachined ultrasonic transducers In air using optical measurements. Ultrasonics Symp. IEEE

1:947–950.
Hedrick WR, Hykes DL, Starchman DE (2004). Ultrasound Physics and Instrumentation. Mosby, 4th edition.
Kocis S, Figura Z (1996). Ultrasonic Measurements and Technologies. Springer, 1st edition.
Ladabaum I, Jin X, Soh HT, Atalar A, Khuri-Yakub BT (1998). Surface micromachined capacitive ultrasonic transducer. IEEE Trans. Ultrasonics, Ferroelectr. Freq. Control 45:678–690.
Ladabaum I, Wagner P, Zanelli C, Mould J, Reynolds P, Wojcik G (2000). Silicon substrate ringing in microfabricated ultrasonic transducers. IEEE Ultrasonics Symp. 1:943–946.
Liu C (2006). Foundations of Mems. Upper Saddle River, Pearson Prentice Hall.
Logan A, Yeow J (2009). Fabricating capacitive micromachined ultrasonic transducers with a novel silicon-nitride-based wafer bonding process. IEEE Trans. Ultrasonic Ferroelectr. Freq. Control 56:1074–084.
Martini S, Bertoli C, Herrera ML, Neeson I, Marangoni A (2005). Attenuation of ultrasonic waves: Influence of microstructures and solid fat content. J. Am. Oil Chem. Soc. 82:319–328.
Raichel D (2006). The Science and Applications of Acoustics. Fort Collins - Springer Science, Business Media.
Wojcik G, Mould J, Reynolds P, Fitzgerald A, Wagner P, Ladabaum I (2000). Time-domain models of MUT array cross-talk in silicon substrates. IEEE Ultrasonic Symp. 1:909–914.